


 Cite this: *RSC Adv.*, 2020, **10**, 15622

# Sarcosenones A–C, highly oxygenated pimarane diterpenoids from an endolichenic fungus *Sarcosomataceae* sp.<sup>†</sup>

 Xintong Hou,<sup>ab</sup> Yang Xu,<sup>b</sup> Shuaiming Zhu,<sup>c</sup> Yang Zhang,<sup>id</sup>\*<sup>c</sup> Liangdong Guo,<sup>d</sup> Feng Qiu<sup>id</sup><sup>a</sup> and Yongsheng Che<sup>\*ab</sup>

Received 17th March 2020

Accepted 6th April 2020

DOI: 10.1039/d0ra02485f

[rsc.li/rsc-advances](http://rsc.li/rsc-advances)

Three new highly oxygenated pimarane diterpenoids, sarcosenones A–C (1–3), and the known 9 $\alpha$ -hydroxy-1,8(14),15-isopimaratrien-3,7,11-trione (4), were isolated from cultures of an endolichenic fungus *Sarcosomataceae* sp. Their structures were elucidated based on NMR spectroscopic data and electronic circular dichroism (ECD) calculations. Compound 1 showed moderate cytotoxicity against a small panel of four human tumor cell lines, with IC<sub>50</sub> values of 7.5–26.4  $\mu$ M.

## Introduction

Pimarane diterpenoids have been encountered as secondary metabolites of higher plants, fungi, and marine organisms.<sup>1</sup> This class of diterpenes can be derived from the original core by substitution, hydroxylation, acetylation, rearrangement, bromination, and ring expansion reactions.<sup>2</sup> Since the isolation of pimaric acid, the first example of this class, in 1839,<sup>3</sup> pimarane diterpenoids have attracted considerable interest due to their remarkable structural diversity and great antimalarial,<sup>4</sup> antibacterial,<sup>5</sup> antifungal,<sup>6</sup> antiviral,<sup>7,8</sup> phytotoxic,<sup>6</sup> cytotoxic,<sup>9–12</sup> AChE-inhibitory,<sup>13</sup> and anti-inflammatory activities.<sup>14</sup>

Sarcosomataceous fungi (Ascomycota), usually known as degraders of wood or as pathogens,<sup>15</sup> have been reported to produce spirobisanaphthalenes,<sup>16,17</sup> lactones,<sup>15,18–21</sup> naphthalones,<sup>21</sup> cyclohexenones,<sup>22</sup> and isocoumarins.<sup>22</sup> Examples include urnucratins A–C with inhibitory effects against methicillin-resistant *Staphylococcus aureus* (MRSA) isolated from *Urnula craterium*,<sup>16</sup> plecillin A with potential anticancer effect isolated from a strain of endolichenic fungus (CGMCC 3.1519216),<sup>17</sup> and galiellalactone derivatives with potent

nematicidal effect, inhibitory activity of IL-6 signalling mediated by SATA3, and cytotoxic activity.<sup>15,19</sup>

Lichens are combinations of a fungus (the mycobiont) and an algal partner (the photobiont or phycobiont). In addition to fungal mycobionts, some nonobligate microfungi, endolichenic fungi, are also found to live asymptotically in the bodies (thalli) of lichens.<sup>23</sup> Endolichenic fungi have been demonstrated to be a rich source of new bioactive natural products.<sup>24</sup> During our continuous search for new cytotoxic metabolites from the endolichenic fungi,<sup>23,25–27</sup> the fungus *Sarcosomataceae* sp. isolated from the lichen *Everniastrum* sp. (Parmeliaceae), which was collected from Zixi Mountain, Yunnan, People's Republic of China, was subjected to chemical investigation. An ethyl acetate (EtOAc) extract of the culture showed cytotoxic effects towards a small panel of four human tumor cell lines. Fractionation of the extract afforded three new highly oxygenated pimarane diterpenoids, which we named sarcosenones A–C (1–3; Fig. 1), and a known analogue 9 $\alpha$ -hydroxy-1,8(14),15-isopimaratrien-3,7,11-trione (4; Fig. 1). Details of the isolation, structure elucidation, and cytotoxicity evaluation of these compounds are reported herein.

## Results and discussion

Sarcosenone A (1) was assigned a molecular formula of C<sub>20</sub>H<sub>24</sub>O<sub>4</sub> (9 degrees of unsaturation) by HRESIMS. Its IR

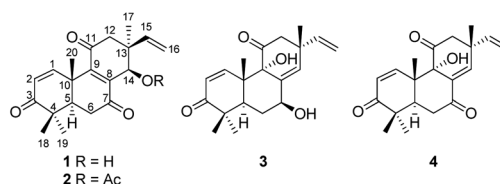


Fig. 1 Structures of compounds 1–4.

<sup>a</sup>Tianjin University of Traditional Chinese Medicine, Tianjin 300193, People's Republic of China

<sup>b</sup>Institute of Medicinal Biotechnology, Chinese Academy of Medical Sciences & Peking Union Medical College, Beijing 100050, People's Republic of China. E-mail: cheys@im.ac.cn

<sup>c</sup>State Key Laboratory of Toxicology & Medical Countermeasures, Beijing Institute of Pharmacology & Toxicology, Beijing 100850, People's Republic of China. E-mail: zhangyang@bmi.ac.cn

<sup>d</sup>State Key Laboratory of Mycology, Institute of Microbiology, Chinese Academy of Sciences, Beijing 100101, People's Republic of China

<sup>†</sup> Electronic supplementary information (ESI) available: UV, IR, CD, HRESIMS, NMR spectra of compounds 1–3; ECD calculations of compounds 1–4. See DOI: 10.1039/d0ra02485f



absorption bands at 3423 and 1677  $\text{cm}^{-1}$  suggested the presence of hydroxyl and carbonyl groups, respectively. Analysis of its NMR data (Table 1) revealed the presence of one exchangeable proton ( $\delta_{\text{H}}$  4.40), four methyl groups, two methylenes, two methines including one oxymethine ( $\delta_{\text{C}}$  68.0), three  $\text{sp}^3$  quaternary carbons, six olefinic carbons with four protonated carbons, and three ketone carbons ( $\delta_{\text{C}}$  199.6, 201.7, and 202.2, respectively). These data accounted for six of the nine degrees of unsaturation calculated from the molecular formula, suggesting that **1** was a tricyclic compound. The  $^1\text{H}$ - $^1\text{H}$  COSY NMR data of **1** showed two isolated spin-systems of C-1-C-2 and C-5-C-6. The  $^1\text{H}$  NMR spectrum displayed signals characteristic for a terminal vinyl group ( $\delta_{\text{H}}$  6.09, dd,  $J = 17.6, 10.9$  Hz, H-15; 5.05, d,  $J = 17.6$  Hz, H-16a; 5.08, d,  $J = 10.9$  Hz, H-16b) and four tertiary methyls ( $\delta_{\text{H}}$  0.98, s, H<sub>3</sub>-17; 1.17, s, H<sub>3</sub>-18; 1.16, s, H<sub>3</sub>-19; 1.59, s, H<sub>3</sub>-20). On the basis of these data, compound **1** should possess the characteristics a pimarane diterpenoid skeleton,<sup>28</sup> which was confirmed by relevant HMBC correlations (Fig. 2). HMBC cross-peaks from H<sub>3</sub>-17 to C-12, C-13, C-14, and C-15, and from H-16 to C-13 indicated that a methyl and a vinyl are both connected to C-13. HMBC correlations from H<sub>3</sub>-20 to C-9 and from H-14 to C-8 and C-9 suggested the presence of a double bond between C-8 and C-9. While those correlations of H-1, H<sub>3</sub>-18, H<sub>3</sub>-19 with C-3, H-5, H-6 $\alpha$ , H-6 $\beta$  with C-7, and of H-12 $\alpha$ , H-12 $\beta$  with C-11 indicated these three carbonyl groups were attached to C-3, C-7, and C-11, respectively. A free hydroxyl

group was located at C-14 by HMBC correlations of H-12 $\alpha$ , H-12 $\beta$  and H<sub>3</sub>-17 to C-14. On the basis of these data, the gross structure of **1** was proposed.

The relative configuration of **1** was proposed by analysis of NOESY data (Fig. 3). NOESY correlations of H-6 $\beta$ /OH-14 and H<sub>3</sub>-18/H<sub>3</sub>-20 implied that OH-14 and Me-20 were both  $\beta$ -oriented, while those of H-5/H<sub>3</sub>-19, H-6 $\alpha$ /H<sub>3</sub>-19 and H-14/H<sub>3</sub>-17 revealed  $\alpha$ -orientation for these protons, thereby establishing the relative configuration of **1**.

The absolute configurations of **1** were deduced by comparison of the experimental and simulated electronic circular dichroism (ECD) spectra calculated using the time-dependent density functional theory (TDDFT).<sup>29</sup> The ECD spectra of the four possible enantiomers **1a-d** (Fig. S11<sup>†</sup>) were calculated. A random conformational analysis was performed for **1a-d** using the MMFF94 force field followed by reoptimization at the B3LYP/6-311G(2d,2p) level, affording the lowest energy conformers (Fig. S11<sup>†</sup>). The overall calculated ECD spectra of **1a-d** were then generated according to Boltzmann weighting of their lowest energy conformers by their relative energies (Fig. 4). The experimental CD spectrum of **1** correlated well to the calculated ECD curve of (5*R*, 10*S*, 13*S*, 14*R*)-**1** (**1a**; Fig. 4), suggesting the 5*R*, 10*S*, 13*S*, 14*R* absolute configuration for **1**.

The molecular formula of sarcosenone B (**2**) was determined to be C<sub>22</sub>H<sub>26</sub>O<sub>5</sub> (10 degrees of unsaturation) based on HRESIMS and the NMR data (Table 1), which is 42 mass units higher than

Table 1 NMR data of 1–3

No.	1		2		3	
	$\delta_{\text{C}}^a$ , type	$\delta_{\text{H}}^b$ ( $J$ in Hz)	$\delta_{\text{C}}^a$ , type	$\delta_{\text{H}}^b$ ( $J$ in Hz)	$\delta_{\text{C}}^c$ , type	$\delta_{\text{H}}^d$ ( $J$ in Hz)
1	154.5, CH	7.78, d (10.5)	154.1, CH	7.78, d (10.5)	152.1, CH	6.81, d (10.4)
2	127.6, CH	5.92, d (10.5)	127.7, CH	5.94, d (10.5)	129.6, CH	5.99, d (10.4)
3	202.2, qC		202.1, qC		203.9, qC	
4	44.6, qC		44.7, qC		44.6, qC	
5	46.8, CH	2.55, dd (15.1, 3.2)	46.9, CH	2.55, dd (15.1, 3.3)	42.1, CH	2.74, dd (13.1, 2.2)
6 $\alpha$	35.6, CH <sub>2</sub>	2.62, dd (17.8, 3.2)	35.5, CH <sub>2</sub>	2.62, dd (17.7, 3.3)	32.7, CH <sub>2</sub>	2.08, m
6 $\beta$		2.80, m		2.78, m		1.59, m
7	199.6, qC		198.2, qC		69.4, CH	4.51, m
8	145.4, qC		141.9, qC		139.9, qC	
9	149.5, qC		152.1, qC		79.3, qC	
10	41.6, qC		41.9, qC		45.0, qC	
11	201.7, qC		201.1, qC		211.6, qC	
12 $\alpha$	46.7, CH <sub>2</sub>	3.11, d (14.7)	46.3, CH <sub>2</sub>	2.34, dd (14.7, 1.2)	53.2, CH <sub>2</sub>	2.67, d (13.3)
12 $\beta$		2.24, d (14.7)		3.13, d (14.7)		2.73, d (13.3)
13	43.8, qC		43.7, qC		43.1, qC	
14	68.0, CH	4.56, s	68.5, CH	5.93, s	129.1, CH	5.95, s
15	144.5, CH	6.09, dd (17.6, 10.9)	143.1, CH	5.86, m	143.2, CH	5.62, dd (17.2, 10.4)
16a	113.3, CH <sub>2</sub>	5.05, d (17.6)	114.2, CH <sub>2</sub>	5.03, d (17.5)	114.3, CH <sub>2</sub>	4.91, d (17.2)
16b		5.08, d (10.9)		5.07, d (10.8)		4.96, d (10.4)
17	22.6, CH <sub>3</sub>	0.98, s	23.2, CH <sub>3</sub>	1.04, s	28.9, CH <sub>3</sub>	1.33, s
18	21.5, CH <sub>3</sub>	1.17, s	21.5, CH <sub>3</sub>	1.17, s	22.6, CH <sub>3</sub>	1.12, s
19	26.9, CH <sub>3</sub>	1.16, s	26.8, CH <sub>3</sub>	1.16, s	28.0, CH <sub>3</sub>	1.22, s
20	23.0, CH <sub>3</sub>	1.59, s	23.2, CH <sub>3</sub>	1.62, s	20.9, CH <sub>3</sub>	1.18, s
21			169.4, qC			
22			21.0, CH <sub>3</sub>	1.91, s		
OH-7						3.44, s
OH-14		4.40, s				

<sup>a</sup> Recorded in acetone-*d*<sub>6</sub> at 150 MHz. <sup>b</sup> Recorded in acetone-*d*<sub>6</sub> at 600 MHz. <sup>c</sup> Recorded in CDCl<sub>3</sub> at 150 MHz. <sup>d</sup> Recorded in CDCl<sub>3</sub> at 600 MHz.



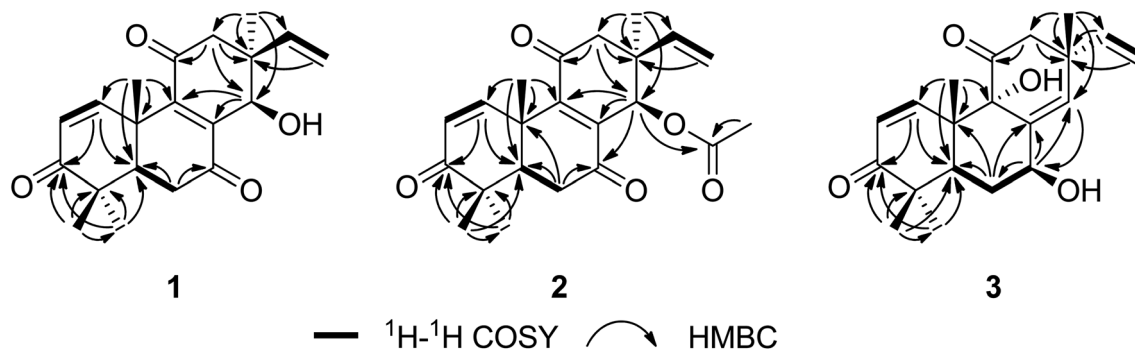


Fig. 2 Key  $^1\text{H}$ - $^1\text{H}$  COSY and HMBC correlations for compounds 1–3.

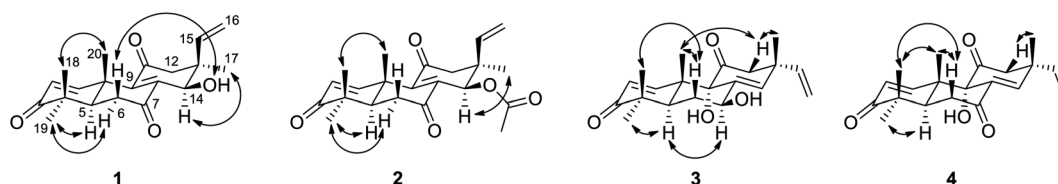


Fig. 3 Key NOESY correlations for compounds 1–4.

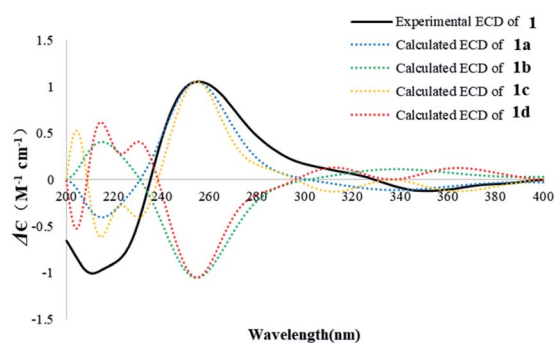


Fig. 4 Experimental ECD spectrum of 1 in MeOH and the calculated ECD spectra of 1a–d.

that of 1. Analysis of the  $^1\text{H}$  and  $^{13}\text{C}$  NMR data for 2 revealed the presence of structural features similar to those found in 1, except that the oxygenated methine proton (H-14) at 4.56 ppm was significantly downfield ( $\delta_{\text{H}}$  5.93). In addition, the NMR resonances corresponding to an acetyl group ( $\delta_{\text{H}}/\delta_{\text{C}}$  1.91/21.0, 169.4) were observed, indicating that the C-14 oxygen of 2 is acylated, which was supported by HMBC cross-peak from H-14 to the carboxylic carbon at 169.4 ppm. On the basis of these data, 2 was determined as the C-14 monoacetate of 1.

The relative configuration of 2 was assigned by analysis of NOESY data and comparison of its  $^1\text{H}$  NMR data with those of sarcosene A (1). NOESY correlation of H<sub>3</sub>-18/H<sub>3</sub>-20 implied that Me-18 and Me-20 were  $\beta$ -oriented, while those of H-5/H<sub>3</sub>-19, H-6 $\alpha$ /H<sub>3</sub>-19, H-12 $\alpha$ /H<sub>3</sub>-17, and H-14/H<sub>3</sub>-17 revealed that the protons were all  $\alpha$ -oriented, establishing the relative configuration of 2.

The absolute configuration of 2 was similarly deduced by comparison of the experimental CD spectrum with the

simulated ECD spectra predicted using the TDDFT at the B3LYP/6-311G(2d,2p) level. The ECD spectra of the four possible isomers 2a–d (Fig. S22<sup>†</sup>) were calculated to represent all possible configurations. The experimental CD spectrum of 2 was nearly identical to that calculated for 2a (Fig. 5), suggesting that 2 has the 5*R*, 10*S*, 13*S*, 14*R* absolute configuration.

Sarcosene C (3) was assigned a molecular formula of C<sub>20</sub>H<sub>26</sub>O<sub>4</sub> (eight degrees of unsaturation) by HRESIMS. Analysis of its NMR data (Table 1) revealed the presence of one exchangeable proton ( $\delta_{\text{H}}$  3.44), four methyl groups, two methylenes, two methines including one oxymethine ( $\delta_{\text{C}}$  69.4), one oxygenated tertiary carbon ( $\delta_{\text{C}}$  79.3), three sp<sup>3</sup> quaternary carbons, six olefinic carbons with five protonated, and two ketone carbons ( $\delta_{\text{C}}$  203.9 and 211.6, respectively). These data accounted for five of the eight degrees of unsaturation calculated from the molecular formula, suggesting that 3 was a tricyclic compound. The  $^1\text{H}$  and  $^{13}\text{C}$  NMR data of 3 revealed structural features closely related to those of a known compound, 9 $\alpha$ -hydroxy-1,8(14),15-isopimaratrien-3,7,11-trione (4).<sup>28</sup> Comparison of the  $^1\text{H}$  and  $^{13}\text{C}$  NMR spectroscopic data of 3 with those of 4 revealed a resonance for one more oxymethine ( $\delta_{\text{H}}/\delta_{\text{C}}$  4.51/69.4) and the absence of signals for a ketone functionality ( $\delta_{\text{C}}$  198.4),<sup>28</sup> suggesting that the carbonyl group at C-7 in 4 was reduced to a hydroxy group. This observation was supported by HMBC correlations from the newly observed H-7 to C-6, C-8, and C-14. Therefore, the gross structure of sarcosene C was proposed as 3.

The relative configuration of 3 was also proposed by analysis of NOESY data (Fig. 3). NOESY correlations of H-6 $\beta$ /H<sub>3</sub>-18, H-6 $\beta$ /H<sub>3</sub>-20, H-12 $\beta$ /H<sub>3</sub>-17 and H-12 $\beta$ /H<sub>3</sub>-20 suggested that Me-17, Me-18, and Me-20 were both  $\beta$ -oriented, while those of H-5/H-7, H-5/H<sub>3</sub>-19 and H-6 $\alpha$ /H-7 revealed that the protons were all  $\alpha$ -oriented. NOESY correlations of H<sub>3</sub>-20 with H-12 $\beta$  and of H-12 $\beta$



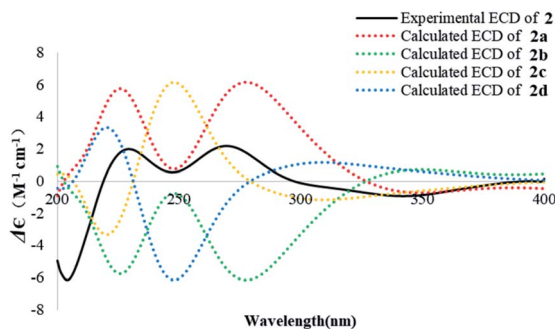


Fig. 5 Experimental ECD spectrum of **2** in MeOH and the calculated ECD spectra of **2a–d**.

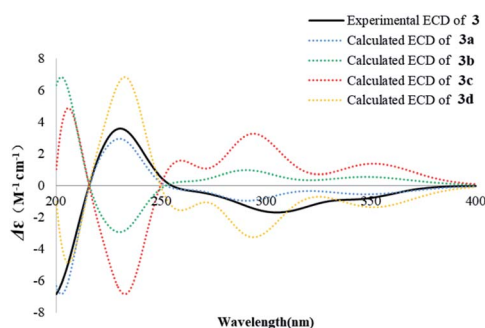


Fig. 6 Experimental ECD spectrum of **3** in MeOH and the calculated ECD spectra of **3a–d**.

with H<sub>3</sub>-17 indicated that these protons are on the same face of the ring system and necessitates  $\alpha$ -orientation for OH-9.<sup>28</sup> Therefore, the relative configuration of **3** was deduced as shown.

The absolute configuration of **3** was also assigned by comparison of the experimental CD spectrum with the simulated ECD spectra generated by excited state calculation using TDDFT. The ECD spectra of the four enantiomers **3a–d** (Fig. S33<sup>†</sup>) were calculated to represent all possible configurations. The MMFF94 conformational search followed by reoptimization at the B3LYP/6-311G(2d,2p) level afforded the lowest-energy conformers (Fig. S33<sup>†</sup>). The overall ECD spectra were then generated according to Boltzmann weighting of each conformer. The CD spectrum of **3** correlated well to the

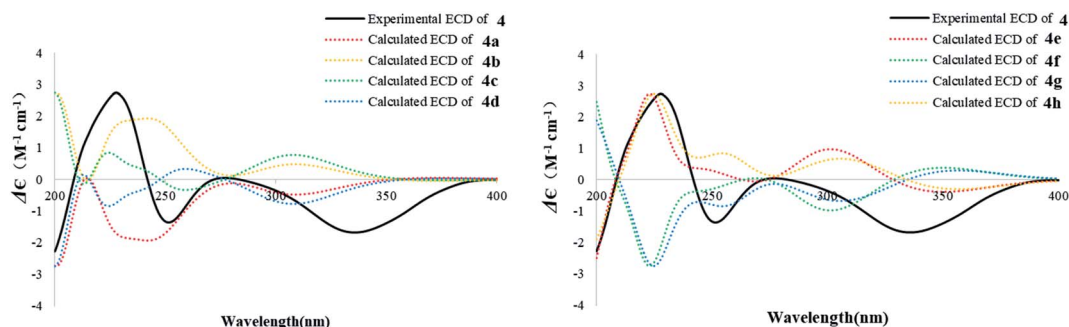


Fig. 7 Experimental ECD spectrum of **4** in MeOH and the calculated ECD spectra of **4a–h**.

Table 2 Cytotoxicity of compound **1**

Compound	IC <sub>50</sub> <sup>a</sup> (μM)			
	MCF-7	HeLa	HepG2	786-O
<b>1</b>	10.3 ± 1.0	11.9 ± 4.4	26.4 ± 3.2	7.5 ± 2.5
Cisplatin <sup>b</sup>	25.7 ± 3.1	29.0 ± 2.5	24.2 ± 3.8	29.2 ± 2.1

<sup>a</sup> IC<sub>50</sub> values were averaged from at least three independent experiments. <sup>b</sup> Positive control.

calculated curve of **3a** (Fig. 6), suggesting the *5R, 7S, 9S, 10S, 13R* absolute configuration.

The known compound **4** was identified as *9α*-hydroxy-1,8(14),15-isopimaratrien-3,7,11-trione by comparison of its MS and NMR data with those reported.<sup>28</sup> Although its relative configuration was assigned by NOE correlations, the absolute configuration remained unsolved. Therefore, the absolute configuration was deduced by comparison of the experimental and calculated ECD spectra for the eight possible enantiomers **4a–h**. The MMFF94 conformational search followed by TDDFT reoptimization at the B3LYP/6-31G(2d,2p) basis set level afforded the lowest energy conformers (Fig. S36<sup>†</sup>). The experimental CD spectrum of **4** was nearly identical to the calculated ECD curve of **4a** (Fig. 7), suggesting the *5R, 9S, 10S, 13R* absolute configuration.

Compounds **1–4** were tested for cytotoxicity against a panel of four human tumor cell lines, MCF-7 (breast cancer), HeLa (cervical carcinoma), HepG2 (hepatocellular carcinoma), and 786-O (renal cell adenocarcinoma). Compound **1** showed moderate cytotoxic effects (Table 2), with IC<sub>50</sub> values of 7.5–26.4 μM (the positive control cisplatin showed IC<sub>50</sub> values of 24.2–29.2 μM). However, compounds **2–4** did not show detectable activity at 50 μM.

## Experimental

### General experimental procedures

Optical rotations were measured on a Rudolph Research Analytical automatic polarimeter, and UV data were recorded on a Shimadzu Biospec-1601 spectrophotometer. CD spectra were recorded on a JASCO J-815 spectropolarimeter. IR data were recorded using a Nicolet Magna-IR 750 spectrophotometer. <sup>1</sup>H and <sup>13</sup>C NMR spectra were acquired with Bruker Avance III-600



spectrometers using solvent signals (acetone- $d_6$ :  $\delta_{\text{H}}$  2.05/ $\delta_{\text{C}}$  29.8, 206.1;  $\text{CDCl}_3$ :  $\delta_{\text{H}}$  7.26/ $\delta_{\text{C}}$  77.2) as references. The HSQC and HMBC experiments were optimized for 145.0 and 8.0 Hz, respectively. ESIMS and HRESIMS data were obtained on an Agilent Accurate-Mass-Q-TOF LC/MS G6550 instrument equipped with an ESI source. HPLC analysis and separation were performed using an Agilent 1260 instrument equipped with a variable-wavelength UV detector.

### Fungal material

The culture of *Sarcosomataceae* sp. was isolated from the lichen *Everniastrum* sp. (Parmeliaceae) collected from Zixi Mountain, Yunnan, People's Republic of China, in November 2006. The fungus was identified by L. G. and assigned the Accession no. 65-7-1-2 in L. G.'s culture collection at the Institute of Microbiology, Chinese Academy of Sciences, Beijing. The fungal strain was cultured on slants of potato dextrose agar (PDA) at 25 °C for 10 days. Agar plugs were cut into small pieces (about  $0.5 \times 0.5 \times 0.5 \text{ cm}^3$ ) under aseptic conditions, and 25 pieces were used to inoculate in five 250 mL Erlenmeyer flasks, each containing 50 mL of media (0.4% glucose, 1% malt extract, and 0.4% yeast extract), and the final pH of the media was adjusted to 6.5 and sterilized by autoclave. Five flasks of the inoculated media were incubated at 25 °C on a rotary shaker at 170 rpm for 5 days to prepare the seed culture. Fermentation was carried out in 10 Fernbach flasks (500 mL) each containing 80 g of rice. Distilled  $\text{H}_2\text{O}$  (120 mL) was added to each flask, and the contents were soaked overnight before autoclaving at 15 psi for 30 min. After cooling to room temperature, each flask was inoculated with 5.0 mL of the spore inoculum and incubated at 25 °C for 40 days.

### Extraction and isolation

The fermentation material was extracted repeatedly with EtOAc ( $4 \times 4.0 \text{ L}$ ), and the organic solvent was evaporated to dryness under vacuum to afford 2.7 g of crude extract. The crude extract was fractionated by silica gel vacuum liquid chromatography (VLC) using petroleum ether–EtOAc–MeOH gradient elution. The fraction (107.5 mg) eluted with 6.5 : 1 petroleum ether–EtOAc was separated by Sephadex LH-20 column chromatography (CC) eluting with 1 : 1  $\text{CH}_2\text{Cl}_2$ –MeOH and the resulting subfractions were combined and purified by semipreparative RP HPLC (Agilent Zorbax SB-C<sub>18</sub> column; 5  $\mu\text{m}$ ;  $9.4 \times 250 \text{ mm}$ ; 47%  $\text{CH}_3\text{CN}$  in  $\text{H}_2\text{O}$  for 30 min;  $2 \text{ mL min}^{-1}$ ) to afford **2** (1.0 mg,  $t_{\text{R}}$  20.0 min). The fraction (165.8 mg) eluted with 3.5 : 1 petroleum ether–EtOAc was separated by reversed-phase silica gel column chromatography (CC) eluting with a MeOH– $\text{H}_2\text{O}$  gradient. The subfraction (18 mg) eluted with 40% MeOH– $\text{H}_2\text{O}$  was purified by semipreparative RP HPLC (Agilent Zorbax SB-C<sub>18</sub> column; 5  $\mu\text{m}$ ;  $9.4 \times 250 \text{ mm}$ ; 37%  $\text{CH}_3\text{CN}$  in  $\text{H}_2\text{O}$  for 30 min;  $2 \text{ mL min}^{-1}$ ) to afford **3** (4.0 mg,  $t_{\text{R}}$  22.5 min). The subfraction (23 mg) eluted with 50% MeOH– $\text{H}_2\text{O}$  was purified by semipreparative RP HPLC (Agilent Zorbax SB-C<sub>18</sub> column; 5  $\mu\text{m}$ ;  $9.4 \times 250 \text{ mm}$ ; 55% MeOH in  $\text{H}_2\text{O}$  for 90 min;  $2 \text{ mL min}^{-1}$ ) to afford **4** (2.7 mg,  $t_{\text{R}}$  67.5 min) and **1** (3.4 mg,  $t_{\text{R}}$  82.5 min).

**Sarcosone A (1).** Colorless oil;  $[\alpha]_{\text{D}}^{25} -127.8$  ( $c$  0.05, MeOH); UV (MeOH)  $\lambda_{\text{max}}$  (log  $\epsilon$ ) 206 (3.82), 223 (3.83) nm; CD ( $c$   $2.0 \times 10^{-4} \text{ M}$ , MeOH)  $\lambda_{\text{max}}$  ( $\Delta\epsilon$ ) 211 (−1.01), 256 (+1.05), 352 (−0.12) nm; IR (neat)  $\nu_{\text{max}}$  3423, 2969, 2926, 1677, 1612, 1395, 1043, 593  $\text{cm}^{-1}$ ;  $^1\text{H}$  and  $^{13}\text{C}$  NMR data see Table 1; HMBC data (acetone- $d_6$ , 600 MHz) H-1  $\rightarrow$  C-3, 5; H-2  $\rightarrow$  C-4, 10; H-5  $\rightarrow$  C-4, 7, 10, 20; H-6 $\alpha$   $\rightarrow$  C-7, 10; H-6 $\beta$   $\rightarrow$  C-5, 7, 10; H-12 $\alpha$   $\rightarrow$  C-11, 13, 14, 15, 17; H-12 $\beta$   $\rightarrow$  C-9, 11, 13, 14, 15, 17; H-14  $\rightarrow$  C-8, 9, 12; H-16a  $\rightarrow$  C-13, 15; H-16b  $\rightarrow$  C-13, 15; H<sub>3</sub>-17  $\rightarrow$  C-12, 13, 14, 15; H<sub>3</sub>-18  $\rightarrow$  C-3, 4, 19; H<sub>3</sub>-19  $\rightarrow$  C-3, 4, 5, 18; H<sub>3</sub>-20  $\rightarrow$  C-1, 5, 9, 10; NOESY correlations (acetone- $d_6$ , 600 MHz) H-5  $\leftrightarrow$  H<sub>3</sub>-19; H-6 $\alpha$   $\leftrightarrow$  H<sub>3</sub>-19; H-6 $\beta$   $\leftrightarrow$  OH-14; H-14  $\leftrightarrow$  H<sub>3</sub>-17; H<sub>3</sub>-18  $\leftrightarrow$  H<sub>3</sub>-20; HRESIMS  $m/z$  329.1749  $[\text{M} + \text{H}]^+$  (calcd for  $\text{C}_{20}\text{H}_{24}\text{O}_4$ , 329.1747).

**Sarcosone B (2).** Colorless oil;  $[\alpha]_{\text{D}}^{25} -47.5$  ( $c$  0.08, MeOH); UV (MeOH)  $\lambda_{\text{max}}$  (log  $\epsilon$ ) 223 (3.93), 246 (3.86) nm; CD ( $c$   $8.0 \times 10^{-4} \text{ M}$ , MeOH)  $\lambda_{\text{max}}$  ( $\Delta\epsilon$ ) 202 (−5.85), 229 (+1.99), 269 (+2.18), 350 (−0.92) nm; IR (neat)  $\nu_{\text{max}}$  3480, 2972, 2935, 1756, 1684, 1370, 1221, 1021, 599, 499  $\text{cm}^{-1}$ ;  $^1\text{H}$  and  $^{13}\text{C}$  NMR data see Table 1; HMBC data (acetone- $d_6$ , 600 MHz) H-1  $\rightarrow$  C-3, 5, 10; H-2  $\rightarrow$  C-10; H-5  $\rightarrow$  C-10; H-6 $\alpha$   $\rightarrow$  C-5, 7, 10; H-6 $\beta$   $\rightarrow$  C-5, 7, 10; H-12 $\alpha$   $\rightarrow$  C-9, 11, 13, 14, 17; H-12 $\beta$   $\rightarrow$  C-11, 13, 14, 17; H-14  $\rightarrow$  C-7, 8, 9, 12, 21; H-16a  $\rightarrow$  C-13, 15; H-16b  $\rightarrow$  C-13, 15; H<sub>3</sub>-17  $\rightarrow$  C-12, 13, 14, 15; H<sub>3</sub>-18  $\rightarrow$  C-3, 4, 5, 19; H<sub>3</sub>-19  $\rightarrow$  C-3, 4, 5, 10, 18; H<sub>3</sub>-20  $\rightarrow$  C-1, 5, 9, 10; H<sub>3</sub>-22  $\rightarrow$  C-21; NOESY correlations (acetone- $d_6$ , 600 MHz) H-5  $\leftrightarrow$  H<sub>3</sub>-19; H-6 $\alpha$   $\leftrightarrow$  H<sub>3</sub>-19; H-12 $\alpha$   $\leftrightarrow$  H-17; H-14  $\leftrightarrow$  H<sub>3</sub>-17; H<sub>3</sub>-18  $\leftrightarrow$  H<sub>3</sub>-20; HRESIMS  $m/z$  393.1670  $[\text{M} + \text{Na}]^+$  (calcd for  $\text{C}_{22}\text{H}_{26}\text{O}_5$ , 393.1672).

**Sarcosone C (3).** Colorless oil;  $[\alpha]_{\text{D}}^{25} -124.4$  ( $c$  0.07, MeOH); UV (MeOH)  $\lambda_{\text{max}}$  (log  $\epsilon$ ) 205 (3.82), 219 (3.79) nm; CD ( $c$   $2.4 \times 10^{-4} \text{ M}$ , MeOH)  $\lambda_{\text{max}}$  ( $\Delta\epsilon$ ) 230 (+3.58), 305 (−1.69) nm; IR (neat)  $\nu_{\text{max}}$  3440, 2963, 2877, 1710, 1666, 1374, 1057, 1035  $\text{cm}^{-1}$ ;  $^1\text{H}$  and  $^{13}\text{C}$  NMR data see Table 1; HMBC data ( $\text{CDCl}_3$ , 600 MHz) H-1  $\rightarrow$  C-3, 5, 9; H-2  $\rightarrow$  C-4; H-5  $\rightarrow$  C-6, 7, 18, 20; H-6 $\alpha$   $\rightarrow$  C-5, 7, 8, 10; H-6 $\beta$   $\rightarrow$  C-5, 7, 8, 10; H-7  $\rightarrow$  C-6, 8, 14; H-12 $\alpha$   $\rightarrow$  C-9, 11, 13, 14, 17; H-12 $\beta$   $\rightarrow$  C-11, 13, 14, 15, 17; H-14  $\rightarrow$  C-7, 9, 12, 13, 17; H-15  $\rightarrow$  C-12, 13, 14, 17; H-16a  $\rightarrow$  C-13, 15; H-16b  $\rightarrow$  C-13; H<sub>3</sub>-17  $\rightarrow$  C-11, 12, 13, 14, 15; H<sub>3</sub>-18  $\rightarrow$  C-3, 4, 5, 19; H<sub>3</sub>-19  $\rightarrow$  C-3, 5, 18; H<sub>3</sub>-20  $\rightarrow$  C-1, 5, 9, 10; NOESY correlations ( $\text{CDCl}_3$ , 600 MHz) H-5  $\leftrightarrow$  H-7; H-5  $\leftrightarrow$  H<sub>3</sub>-19; H-6 $\alpha$   $\leftrightarrow$  H-7; H-6 $\beta$   $\leftrightarrow$  H<sub>3</sub>-18; H-6 $\beta$   $\leftrightarrow$  H<sub>3</sub>-20; H-12 $\beta$   $\leftrightarrow$  H-17; H-12 $\beta$   $\leftrightarrow$  H-20; HRESIMS  $m/z$  331.1908  $[\text{M} + \text{H}]^+$  (calcd for  $\text{C}_{20}\text{H}_{26}\text{O}_4$ , 331.1904).

### Computational details

Conformational analyses for **1–4** were performed *via* the Molecular Operating Environment (MOE) version 2009.10 (Chemical Computing Group, Canada) software package with LowModeMD at the MMF94 force field. The MMF94 conformers were further optimized using TDDFT at the B3LYP/6-311G(2d,2p) basis set level in MeOH with the IEFPCM model. The stationary points have been checked as the true minima of the potential energy surface by verifying that they do not exhibit vibrational imaginary frequencies. The 25 lowest electronic transitions were calculated, and the rotational strengths of each electronic excitation were given using both dipole length and velocity representations. ECD spectra were simulated in SpecDis23 (ref. 30) using a Gaussian function with half-bandwidths



of 0.30 eV. The overall ECD spectra were then generated according to Boltzmann weighting of each conformer. The systematic errors in the prediction of wavelength and excited-state energies are compensated by employing UV correlation. All quantum computations were performed using the Gaussian 09 package.<sup>31</sup>

### Cytotoxicity assays

The cytotoxic activity of compounds 1–4 were tested using 96 well plates according to a literature MTS method with slight modification.<sup>32</sup> Cells were seeded in 96-well plates at a density of  $1.0 \times 10^4$  cells per well in 100  $\mu$ L of complete culture medium. After cell attachment overnight, the medium was removed, and each well was treated with 100  $\mu$ L of medium containing 0.1% DMSO or appropriate concentrations of the test compounds and the positive control cisplatin and incubated with cells at 37 °C for 48 h in a 5% CO<sub>2</sub>-containing incubator. Proliferation was assessed by adding 20  $\mu$ L of MTS (Promega) to each well in the dark, after 90 min of incubation at 37 °C. The optical density was recorded on a microplate reader at 490 nm. Three duplicate wells were used for each concentration, and all the tests were repeated three times.

### Conclusions

In summary, three new highly oxygenated pimarane diterpenoids, sarcosonones A–C (1–3), and a structurally related known compound (4) were isolated from cultures of *Sarcosomataceae* sp., an endolichenic fungus found in the lichen *Everniastrum* sp. (Parmeliaceae). Their structures were elucidated based on NMR spectroscopic data and electronic circular dichroism (ECD) calculations. The absolute configuration of known compound 4 was determined for the first time. To our knowledge, this is the first report of pimarane diterpenoids isolated from the family *Sarcosomataceae*. Compound 1 showed moderate cytotoxicity, with IC<sub>50</sub> values of 7.5–26.4  $\mu$ M. Theoretically, 1–4 could be generated from the precursor (*E,E,E*)-geranylgeranyl diphosphate (GGDP).<sup>33</sup> GGPP was first cyclized by copalyl diphosphate (CPP) synthases, and then CPP was completely cyclized by pimaradiene synthases, leading to the formation of these metabolites (Scheme S1†).

### Conflicts of interest

The authors declare no conflict of interest.

### Acknowledgements

X. H., S. Z., and Y. Z. were supported in part by the National Program of Drug Research and Development (2012ZX09301-003); Y. X. and Y. C. was supported by the CAMS Innovation Fund for Medical Sciences (2018-I2M-3-005).

### Notes and references

1 P. Reveglia, A. Cimmino, M. Masi, P. Nocera, N. Berova, G. Ellestad and A. Evidente, *Chirality*, 2018, **30**, 1–20.

- X. Wang, H. Yu, Y. Zhang, X. Lu, B. Wang and X. Liu, *Chem. Biodiversity*, 2008, **15**, e1700276.
- S. Palkin, *J. Chem. Educ.*, 1935, **12**, 35–40.
- S. Thongnest, C. Mahidol, S. Sutthivaiyakit and S. Ruchirawat, *J. Nat. Prod.*, 2005, **68**, 1632–1636.
- A. Ulubelen, G. Topcu and C. B. Johansson, *J. Nat. Prod.*, 1997, **60**, 1275–1280.
- A. Andolfi, L. Maddau, S. Basso, B. T. Linaldeddu, A. Cimmino, B. Scanu, A. Deidda, A. Tuzi and A. Evidente, *J. Nat. Prod.*, 2014, **77**, 2352–2360.
- Y. P. Tan, Y. Xue, A. I. Savchenko, S. D. Houston, N. Modhiran, C. L. D. Mcmillan, G. M. Boyle, P. V. Bernhardt, P. R. Young, D. Watterson and C. M. Williams, *J. Nat. Prod.*, 2019, **82**, 2828–2834.
- S. Huang, Q. Ma, W. Fang, F. Xu, H. Peng, H. Dai, J. Zhou and Y. Zhao, *J. Asian Nat. Prod. Res.*, 2013, **7**, 750–755.
- L. Sun, D. Li, M. Tao, Y. Chen, F. Dan and W. Zhang, *Mar. Drugs*, 2012, **10**, 539–550.
- H. Yu, X. Wang, Y. Zhang, W. Xu, J. Zhang, X. Zhou, X. Lu, X. Liu and B. Jiao, *J. Nat. Prod.*, 2018, **81**, 1553–1560.
- U. K. Karmakar, N. Ishikawa, M. A. Arai, F. Ahmed, T. Koyano, T. Kowithayakorn and M. Ishibashi, *J. Nat. Prod.*, 2016, **79**, 2075–2082.
- X. Wang, B. P. Bashyal, E. M. K. Wijeratne, J. M. U'Ren, M. X. Liu, M. K. Gunatilaka, A. E. Arnold and A. A. L. Gunatilaka, *J. Nat. Prod.*, 2011, **74**, 2052–2061.
- S. Huang, H. Luo, Q. Ma, H. Peng, H. Dai, J. Zhou and Y. Zhao, *Chem. Biodiversity*, 2014, **11**, 1406–1416.
- R. Chokchaisiri, W. Chaichompoo, W. Chunklok, S. Cheenpracha, L. Ganranoo, N. Phutthawong, S. Bureekaew and A. Suksamrarn, *J. Nat. Prod.*, 2020, **83**, 14–19.
- B. Köpcke, R. W. S. Weber and H. Anke, *Phytochemistry*, 2002, **60**, 709–714.
- X. Liu, W. R. Schwan, T. J. Volk, M. Rott, M. Liu, P. Huang, Z. Liu, Y. Wang, N. C. Zitomer, C. Sleger, S. Hartsel, A. Monte and L. Zhang, *J. Nat. Prod.*, 2012, **75**, 1534–1538.
- J. Li, R. Ding, H. Gao, L. Guo, X. Yao, Y. Zhang and J. Tang, *RSC Adv.*, 2019, **9**, 39082–39089.
- M. Johansson, B. Köpcke, H. Anke and O. Sterner, *J. Antibiot.*, 2002, **55**, 104–106.
- J. Tian, R. Yu, X. Li, H. Gao, L. Guo, Y. Li, J. Li, J. Tang and X. Yao, *Fitoterapia*, 2015, **101**, 92–98.
- J. Tian, R. Yu, X. Li, H. Gao, L. Guo, J. Tang and X. Yao, *Magn. Reson. Chem.*, 2015, **53**, 861–871.
- W. A. Ayer, L. S. Trifonov, L. J. Hutchison and P. Chakravarty, *Nat. Prod. Lett.*, 2000, **14**, 405–410.
- J. Tian, R. Yu, X. Li, H. Gao, D. Hu, L. Guo, J. Tang and X. Yao, *J. Asian Nat. Prod. Res.*, 2015, **17**, 550–558.
- F. Zhang, L. Li, S. Niu, Y. Si, L. Guo, X. Jiang and Y. Che, *J. Nat. Prod.*, 2012, **75**, 230–237.
- J. J. Kellogg and H. A. Raja, *Phytochem. Rev.*, 2017, **16**, 271–293.
- Y. Wang, S. Niu, S. Liu, L. Guo and Y. Che, *Org. Lett.*, 2010, **12**, 5081–5083.
- F. Zhang, S. Liu, X. Lu, L. Guo, H. Zhang and Y. Che, *J. Nat. Prod.*, 2009, **72**, 1782–1785.



- 27 Y. Wang, Z. Zheng, S. Liu, H. Zhang, E. Li, L. Guo and Y. Che, *J. Nat. Prod.*, 2010, **73**, 920–924.
- 28 J. A. Findlay, G. Li and P. E. Penner, *J. Nat. Prod.*, 1995, **58**, 197–200.
- 29 S. Zhu, F. Ren, Z. Guo, J. Liu, X. Liu, G. Liu and Y. Che, *J. Nat. Prod.*, 2019, **82**, 462–468.
- 30 T. Bruhn, A. Schaumlöffel, Y. Hemberger and G. Bringmann, *Chirality*, 2013, **25**, 243–249.
- 31 M. J. Frisch, G. W. Trucks, H. B. Schlegel, G. E. Scuseria, M. A. Robb, J. R. Cheeseman, G. Scalmani, V. Barone, B. Mennucci, G. A. Petersson, H. Nakatsuji, M. Caricato, X. Li, H. P. Hratchian, A. F. Izmaylov, J. Bloino, G. Zheng, J. L. Sonnenberg, M. Hada, M. Ehara, K. Toyota, R. Fukuda, J. Hasegawa, M. Ishida, T. Nakajima, Y. Honda, O. Kitao, H. Nakai, T. Vreven, J. A. Montgomery Jr, J. E. Peralta, F. Ogliaro, M. Bearpark, J. J. Heyd, E. Brothers, K. N. Kudin, V. N. Staroverov, R. Kobayashi, J. Normand, K. Raghavachari, A. Rendell, J. C. Burant, S. S. Iyengar, J. Tomasi, M. Cossi, N. Rega, J. M. Millam, M. Klene, J. E. Knox, J. B. Cross, V. Bakken, C. Adamo, J. Jaramillo, R. Gomperts, R. E. Stratmann, O. Yazyev, A. J. Austin, R. Cammi, C. Pomelli, J. W. Ochterski, R. L. Martin, K. Morokuma, V. G. Zakrzewski, G. A. Voth, P. Salvador, J. J. Dannenberg, S. Dapprich, A. D. Daniels, O. Farkas, J. B. Foresman, J. V. Ortiz, J. Cioslowski and D. J. Fox, *Gaussian 09, Rev D.01*, Gaussian, Inc.: Wallingford, CT, 2009.
- 32 N. Zhang, Y. Chen, R. Jiang, E. Li, X. Chen, Z. Xi, Y. Guo, X. Liu, Y. Zhou, Y. Che and X. Jiang, *Autophagy*, 2011, **7**, 598–612.
- 33 M. Xu, M. L. Hillwig, M. S. Tiernan and R. J. Peters, *J. Nat. Prod.*, 2017, **80**, 328–333.

